Exchange Processes in Complexes with Two Ruthenium (η^2-Silane) Linkages: Role of the Secondary Interactions between Silicon and Hydrogen Atoms

Isabelle Atheaux,[†] Fabien Delpech,[†] Bruno Donnadieu,[†] Sylviane Sabo-Etienne,*,[†] Bruno Chaudret,[†] Khansaa Hussein,[‡,⊥] Jean-Claude Barthelat,[‡] Thomas Braun,[§] Simon B. Duckett,[§] and Robin N. Perutz[§]

Laboratoire de Chimie de Coordination du CNRS, 205 Route de Narbonne, 31077 Toulouse Cedex 04, France, Laboratoire de Physique Quantique, IRSAMC (UMR 5626), Université Paul Sabatier, 118 Route de Narbonne, 31062 Toulouse Cedex 4, France, and Department of Chemistry, University of York, Heslington, York, YO10 5DD, U.K.

NMR studies and DFT calculations (B3LYP) are used to elucidate the mechanisms for the hydride/(η^2-Si-H) hydrogen exchange observed in the bis(silane) complexes RuH$_2$[(η^2-HSiMe$_2$)$_2$(CH$_2$)$_2$](PCy$_3$)$_2$ (**2**) and RuH$_2$[(η^2-HSiPh$_2$)$_2$O](PCy$_3$)$_2$ (**4**) obtained from the reactions of the bis(dihydrogen) ruthenium complex RuH$_2$(H$_2$)$_2$(PCy$_3$)$_2$ (**1**) with the corresponding disilane HMe$_2$Si(CH$_2$)$_2$SiMe$_2$H or disiloxane HSiPh$_2$OSiPh$_2$H. Evidence is presented that exchange in **2** occurs via formation of isomers with dihydrogen ligands. Conversion of the most stable isomer **A** with C_{2v} symmetry to the asymmetric Ru(η^2-SiH)$_2$ isomer **B** is the prelude to formation of the Ru(η^2-SiH)(η^2-H$_2$) isomer **C** and the Ru(η^2-H$_2$)$_2$ isomer **D**. Exchange occurs via rotation of the dihydrogen ligands and reversal of the isomerization process. The transformation of **A** into **B** via **TS$_{AB}$** is the most energetically demanding individual step. This corresponds to the breaking of the SISHA (secondary interactions between silicon and hydrogen atoms) interactions between the silicons and the classical hydrides Hb and Hc. The calculated barrier of 43 kJ/mol for the complex with H$_3$SiCH$_2$CH$_2$SiH$_3$ and PH$_3$ ligands compares to the experimental enthalpy of activation of 77 ± 11 kJ/mol for **2**. Whereas complex **2** adopts a geometry with C_{2v} symmetry, low-temperature NMR spectroscopy shows that complex **4** is present as two isomers, an asymmetric isomer with C_1 symmetry and the symmetric isomer in proportions of ca. 1:2. The pathways for interconversion of the isomers and for exchange between the hydride and SiH hydrogen atoms have been delineated by DFT calculations and resemble those for complex **2**. Reaction of **4** with excess triphenylphosphine yields RuH$_2${(η^2-H-SiPh$_2$)O(SiHPh$_2$)}(PPh$_3$)$_3$ (**5**), which is shown by NMR spectroscopy to contain one coordinated and one uncoordinated SiH group. A crystal structure of the partially hydrolyzed analogue RuH$_2${(η^2-H-SiPh$_2$)O(Si(OH)Ph$_2$)}(PPh$_3$)$_3$ (**6**) confirms the assignment. A ruthenium(II) formulation with one (η^2-SiH) bond and two SISHA interactions is favored over a ruthenium(IV) structure with three hydrides and a silyl ligand.

Introduction

The chemistry of σ-complexes resulting from the coordination of a H−E bond (E = H, Si, B, C) of a substrate to a metal center has excited great interest over the last 15 years.[1] Dihydrogen complexes represent the most studied family and are known with a range of different H−H distances, indicating that, in principle, any stage may be isolated between the initial coordination of H$_2$ and the final oxidative addition of H$_2$. Additional dihydrogen interactions may be present between a hydride and another hydrogen in the coordination sphere of the metal.[2] The differences between these complexes are often very slight, and a combination of different techniques is required to obtain a complete view of the nature of the bonding. For this purpose, NMR studies associated with deuteration experiments, X-ray structure determination (or neutron diffraction), and theoretical calculations prove to be complementary. In addition to the fundamental understanding, knowledge of structure and dynamics is important in order

---

(1) (a) Kubas, G. J. *Metal Dihydrogen and σ-Bond Complexes*; Kluwer Academic/Plenum Publishers: New York, 2001. (b) Hall, C.; Perutz, R. N. *Chem. Rev.* **1996**, *96*, 3125.

(2) (a) Kubas, G. J. *Acc. Chem. Res.* **1988**, *21*, 120. (b) Crabtree, R. H. *Acc. Chem. Res.* **1990**, *23*, 95. (c) Jessop, P. G.; Morris, R. H. *Coord. Chem. Rev.* **1992**, *121*, 155. (d) Heinekey, D. M.; Oldham, W. J., Jr. *Chem. Rev.* **1993**, *93*, 913. (e) Crabtree, R. H. *Angew. Chem., Int. Ed. Engl.* **1993**, *32*, 789. (f) Esteruelas, M. A.; Oro, L. A. *Chem. Rev.* **1998**, *98*, 577. (f) Crabtree, R. H.; Siegbahn, P. E. M.; Eisenstein, O.; Rheingold, A. L.; Koetzle, T. F. *Acc. Chem. Res.* **1996**, *29*, 348. (g) Maseras, F.; Lledós, A.; Clot, E.; Eisenstein, O. *Chem. Rev.* **2000**, *100*, 601.

Scheme 1

X = (CH₂)₂, (**2**); (C₆H₄), (**3**)
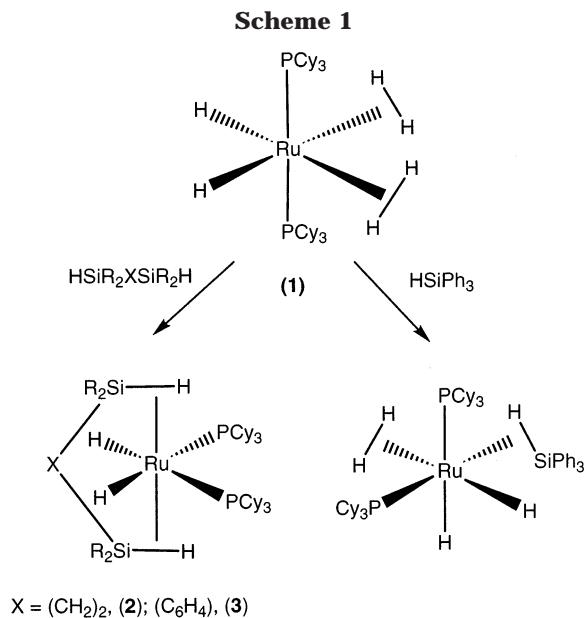
to induce a specific reaction or control the selectivity in a catalytic process.

The same approach can be followed when considering the silane family. Unstretched and stretched complexes have been isolated and display different reactivity.[3] Our group is currently involved in investigations based on the activation of silanes by the ruthenium bis(dihydrogen) precursor $RuH_2(H_2)_2(PCy_3)_2$ (**1**).[4−7] In particular, we have shown that complexes with two σ-bonds can be synthesized. One family of complexes, of general formula $RuH_2\{(H\text{-}SiR_2)_2X\}(PR_3)_2$, contains two coordinated σ-Si−H bonds from a disilane ligand,[5] while one σ-Si−H and one σ-H−H bond are found in $RuH_2(\sigma\text{-}H_2)$-$(\sigma\text{-}H\text{-}SiPh_3)(PCy_3)_2$ (Scheme 1).[6] X-ray data were obtained for several complexes and are in very good agreement with DFT calculations. Both studies highlighted the importance of secondary interactions between the silicon atoms and all the hydrogen atoms present in the coordination sphere of the metal.[5,6] These Si···H interactions, subsequently denoted SISHA (secondary interactions between silicon and hydrogen atoms), are characterized by distances in the range 2.0−2.5 Å. They are responsible for the stability of the complexes and for the *cis* geometry of the two phosphine ligands even in the case of the bulky PCy₃.

We have already reported preliminary data on the dynamic behavior of these complexes.[5] Exchange between the two types of hydrogen in $RuH_2\{(H\text{-}SiR_2)_2X\}$-

$(PR_3)_2$ occurs with barriers between 47 and 69 kJ/mol according to the nature of the disilane. A literature survey demonstrates the complexity of the exchange processes in σ-silane complexes.[8−13] Several mechanisms are postulated in which oxidative addition and reductive elimination steps play a major role. An equilibrium between a hydrido(silyl) or a σ-silane species is often invoked, implying the intermediacy of a dihydrogen species in some cases. The situation is even more complicated when dihydrogenosilanes are used, as additional exchange pathways can occur between the hydride and the silicon-attached hydrogen.

We now describe an in-depth NMR and theoretical study of the mechanism of the exchange processes on two different bis(silane) complexes. We also report the isolation and characterization of a new complex with a pendant Si−H group. The role of the Si···H interactions (SISHA) is particularly emphasized.

Results and Discussion

Symmetrical Bis(silane) Complex $RuH_z[(\eta^2\text{-}HSi\text{-}Me_2)_2(CH_2)_2](PCy_3)_2$. The bis(silane) complex $RuH_2[(\eta^2\text{-}HSiMe_2)_2(CH_2)_2](PCy_3)_2$ (**2**) was previously isolated from the reaction of the bis(dihydrogen) ruthenium complex **1** with $HMe_2Si(CH_2)_2SiMe_2H$.[5] Complex **2** has been characterized by X-ray diffraction and, like other members of the bis(silane) family, displays a *cis* orientation for the two phosphines, each *trans* to a hydride with the hydrogen atoms of the bis(silane) ligand lying *trans* to one another (Scheme 1). The two $(\eta^2\text{-}Si\text{-}H)$ bond lengths are 1.73(3) and 1.78(4) Å, whereas the distances between the silicon atoms and the hydrides are 2.12-(3), 2.13(3), 2.27(3), and 2.31(3) Å. We have already reported DFT studies on the series of bis(silane) complexes and have shown that for a disilane with two or three atoms bridging the two silicon atoms the most stable isomer corresponds to a species with a symmetrical arrangement of the disilane ligand in perfect agreement with the X-ray structures.[5b] For example, in the case of **2**, the X-ray distances compare well with those obtained by DFT calculation for the isomer RuH_2-$[(\eta^2\text{-}HSiH_2)_2(CH_2)_2](PH_3)_2$ (1.853 Å for the two $(\eta^2\text{-}Si\text{-}H)$ bonds and 2.220 and 2.329 Å for the nonbonding Si···H distances).[5b] It was demonstrated previously that only trivial differences are found when the hybrid

(3) (a) Corey, J. Y.; Braddock-Wilking, J. *Chem. Rev.* **1999**, *99*, 175. (b) Schubert, U. *Adv. Organomet. Chem.* **1990**, *30*, 151. (c) Lin, Z. *Chem. Soc. Rev.* **2002**, *31*, 2399.
(4) (a) Christ, M. L.; Sabo-Etienne, S.; Chaudret, B. *Organometallics* **1995**, *14*, 1082. (b) Delpech, F.; Sabo-Etienne, S.; Donnadieu, B.; Chaudret, B. *Organometallics* **1998**, *17*, 4926. (c) Delpech, F.; Mansas, J.; Leuser, H.; Sabo-Etienne, S.; Chaudret, B. *Organometallics* **2000**, *19*, 5750.
(5) (a) Delpech, F.; Sabo-Etienne, S.; Chaudret, B.; Daran, J.-C. *J. Am. Chem. Soc.* **1997**, *119*, 3167. (b) Delpech, F.; Sabo-Etienne, S.; Daran, J.-C.; Chaudret, B.; Hussein, K.; Marsden, C. J.; Barthelat, J.-C. *J. Am. Chem. Soc.* **1999**, *121*, 6668.
(6) Hussein, K.; Marsden, C. J.; Barthelat, J.-C.; Rodriguez, V.; Conejero, S.; Sabo-Etienne, S.; Donnadieu, B.; Chaudret, B. *Chem. Commun.* **1999**, 1315.
(7) Atheaux, I.; Donnadieu, B.; Rodriguez, V.; Sabo-Etienne, S.; Chaudret, B.; Hussein, K.; Barthelat, J.-C. *J. Am. Chem. Soc.* **2000**, *122*, 5664.

(8) Luo, X. L.; Crabtree, R. H. *J. Am. Chem. Soc.* **1989**, *111*, 2527.
(9) (a) Wang, W. D.; Eisenberg, R. *Organometallics* **1992**, *11*, 908. (b) Fryzuk, M. D.; Rosenberg, L.; Rettig, S. J. *Organometallics* **1991**, *10*, 2537. (c) Fryzuk, M. D.; Rosenberg, L.; Rettig, S. J. *Organometallics* **1996**, *13*, 2871. (d) Fryzuk, M. D.; Rosenberg, L.; Rettig, S. J. *Inorg. Chim. Acta* **1994**, *222*, 345. (e) Heyn, R. H.; Huffman, J. C.; Caulton, K. G. *New J. Chem.* **1993**, *17*, 797. (f) Schubert, U.; Gilbert, S.; Mock, S. *Chem. Ber.* **1992**, *125*, 835.
(10) (a) Duckett, S. B.; Perutz, R. N. *J. Chem. Soc., Chem. Commun.* **1991**, 28. (b) Scharrer, E.; Chang, S.; Brookhart, M. *Organometallics* **1995**, *14*, 5686. (c) Muhoro, C. N.; Xiaoming, H.; Hartwig, J. F. *J. Am. Chem. Soc.* **1999**, *121*, 5033.
(11) (a) Esteruelas, M. A.; Oro, L. A.; Valero, C. *Organometallics* **1991**, *10*, 462. (b) Maseras, F.; Lledós, A. *Organometallics* **1996**, *15*, 1218. (c) Luo, X. L.; Kubas, G. J.; Burns, C. J.; Bryan, J. C.; Unkefer, C. J. *J. Am. Chem. Soc.* **1995**, *117*, 1159. (d) Ng, S. M.; Lau, C. P.; Fan, M. F.; Lin, Z. *Organometallics* **1999**, *18*, 2484.
(12) (a) Aitken, C. T.; Harrod, J. F.; Samuel, E. *J. Am. Chem. Soc.* **1986**, *108*, 4059. (b) Harrod, J. F.; Mu, Y.; Samuel, E. *Can. J. Chem.* **1992**, *70*, 2980. (c) Hao, L.; Lebuis, A. M.; Harrod, J. F.; Samuel, E. *J. Chem. Soc., Chem. Commun.* **1997**, 2193.
(13) (a) Suzuki, H.; Takao, T.; Tanaka, M.; Moro-oka, Y. *J. Chem. Soc., Chem. Commun.* **1992**, 476. (b) Takao, T.; Suzuki, H.; Tanaka, M. *Organometallics* **1994**, *13*, 2554. (c) Takao, T.; Yoshida, S.; Suzuki, H.; Tanaka, M. *Organometallics* **1995**, *14*, 3855.

Table 1. Rate Constants for Hydrides/(η^2-Si–H) Protons Exchange at Given Temperatures

T (K)	k (s^{-1}) (1D-NOE)	k (s^{-1}) (2D-NOESY)
297.1	0.88	1.86
305.5	2.33	2.79
316.6	7.32	7.46
332.8	28.2	34.8

functional B3LYP is replaced by B3PW91. It was also verified that the replacement of the alkyl groups on both silicon and phosphorus atoms did not induce any significant change.

The ^{1}H NMR spectrum of **2** shows two high-field resonances at room temperature. The triplet at δ -8.21 is attributed to the two (η^2-Si–H) protons and the multiplet at δ -12.65 to the two classical hydrides. The spectra are temperature-dependent, and coalescence of the two signals is obtained at 376 K. The free energy of activation for exchange of 68.4 kJ/mol is calculated from the rate of exchange at the coalescence temperature. The relaxation time T_1 of the SiH and hydride protons has been determined as ca. 300 ms at 195 K.
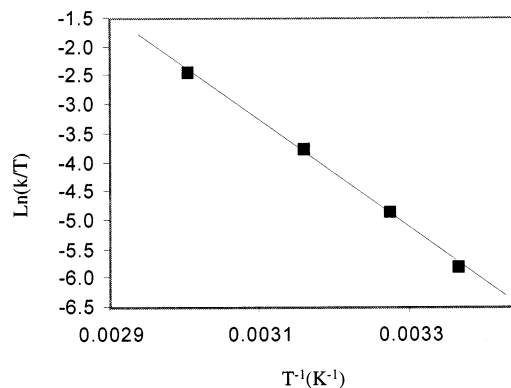
We have now studied complex **2** by NOESY and EXSY methods in order to extend the temperature range and obtain further mechanistic details of the exchange process. At 273 K and below, NOESY/EXSY spectra (at 400 MHz) showed negative NOE cross-peaks between the hydride and (η^2-Si–H) protons, which indicates that exchange was negligible at this temperature. In contrast, when EXSY spectra were recorded in toluene-d_8 between 297 and 333 K, with mixing times of 20, 50, and 100 ms, positive cross-peaks were observed between the resonances. The rate constants for exchange between these sites were then determined by the matrix method (Table 1).[14]

Faster, one-dimensional NOE NMR experiments were carried at four different temperatures to provide an independent set of rate data. Rate constants were derived by use of the equation for a two-spin exchange process (eq 1),[14]

$$k\tau_{\mathrm{m}} = -0.5\,\ln(I-1)/(I+1) \tag{1}$$

where k is the rate constant for exchange, τ_{m} is the mixing time, and $I = I_A/I_B$ corresponds to the ratio of peak areas. The activation parameters obtained from the Eyring analysis (Figure 1) are $\Delta H^\ddagger = 77 \pm 11$ kJ/mol and $\Delta S^\ddagger = 14 \pm 34$ J/K^{-1} mol^{-1}. The entropy of activation for this rearrangement is close to zero, indicative of an intramolecular process. The free energy of activation is calculated to be 72 kJ/mol at 376 K, in acceptable agreement with the barrier derived from the coalescence temperature (68.4 kJ/mol).

The NMR results are consistent with the proximity of the (η^2-Si–H) protons and the hydrides (SISHA interactions) allowing an intramolecular exchange process. Several mechanisms can be proposed for the exchange process, and we have investigated three different pathways. The complex is saturated and exchange could occur via (i) phosphine dissociation; (ii) formation of dihydrogen isomers; or (iii) generation of a dangling Si–H bond.

(14) (a) Perrin, C. L.; Gipe, R. K. *J. Am. Chem. Soc.* **1984**, *106*, 4036. (b) Perrin, C. L.; Dwyer, T. J. *Chem. Rev.* **1990**, *90*, 935.

Figure 1. Eyring plot showing the temperature dependence of the rate of exchange between the hydrides and the (η^2-Si–H) protons for **2**.
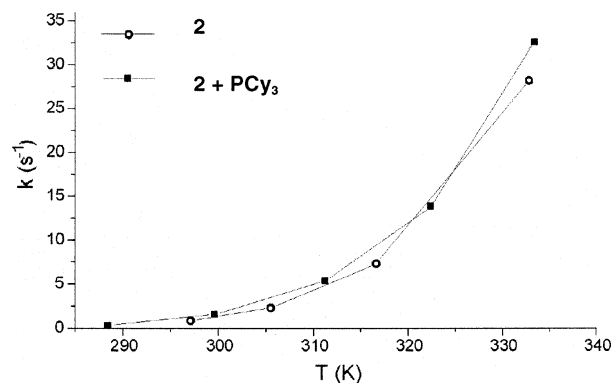
Figure 2. Plot of observed rate constants for exchange between the hydrides and the (η^2-Si–H) protons for **2** with (or without) 1 equiv of PCy$_3$ as a function of temperature.

Mechanism (i): Phosphine Dissociation. The small value found for the entropy of activation argues against mechanism (i) involving phosphine dissociation. This conclusion was also confirmed by NMR and DFT data. We have performed 1D NOE NMR experiments on a toluene-d_8 solution of **2** in the presence of 1 equiv of PCy$_3$ and determined the rate constant for exchange as a function of temperature. The plots of k vs T for a solution of **2** and a solution of **2** + PCy$_3$ are very similar (Figure 2). The absence of change in rate constant clearly excludes phosphine dissociation.

We have used the model complex RuH$_2$[(η^2-HSiH$_2$)$_2$-(CH=CH)](PH$_3$)$_2$ (**A**) to analyze the exchange process by DFT calculations.[15] The B3LYP-optimized geometry of **A** is displayed in Figure 3, and the calculated geometrical parameters are listed in Table 2. The complex resulting from PH$_3$ dissociation was optimized and found to lie 129.8 kJ/mol above **A**, far above the experimental value of the exchange barrier. This process is thus energetically unfavorable and can be definitively ruled out.

Mechanism (ii): Dihydrogen Isomers. In a mechanism involving the intermediacy of dihydrogen species, the multiple interactions between the silicon atoms and the hydrogen atoms should play a major role. Although we have no direct evidence of the intermediacy of a dihydrogen species, this hypothesis is consistent with the observations made during the exposure of the bis-(silane) complexes to a dihydrogen or deuterium atmo-

(15) Fan, M.-F.; Lin, Z. *Organometallics* **1999**, *18*, 286.

Table 2. Selected Geometrical Parameters for the Various Isomers and Transition States Involved in Mechanism (ii)

	2 X-ray	A DFT	TS$_{AB}$	B	TS$_{BC}$	C	TS$_{CD}$	D	TS$_{rotDab}$	TS$_{rotDcd}$
Si1–Ha	1.73(3)	1.850	1.821	1.794	1.879	1.970	2.256	2.681	3.103	2.639
Si1–Hb	2.27(3)	2.259	3.625	3.511	3.570	3.617	3.399	3.394	3.105	3.369
Si2–Hc	2.13(3)	2.259	3.263	3.565	3.507	3.441	2.654	2.787	2.783	2.564
Si2–Hd	1.78(4)	1.850	1.706	2.131	2.466	2.731	3.362	3.068	2.894	3.251
Ru–Ha	1.55(3)	1.682	1.650	1.633	1.624	1.618	1.625	1.783	1.834	1.764
Ru–Hb	1.60(3)	1.631	1.612	1.645	1.647	1.651	1.657	1.804	1.839	1.787
Ru–Hc	1.50(3)	1.631	1.643	1.607	1.614	1.709	1.718	1.722	1.702	1.728
Ru–Hd	1.54(3)	1.682	1.661	1.620	1.621	1.718	1.723	1.741	1.726	1.744
Ru–Si1	2.4282(6)	2.428	2.519	2.506	2.486	2.474	2.456	2.465	2.459	2.454
Ru–Si2	2.4109(7)	2.428	2.535	2.494	2.503	2.511	2.507	2.441	2.430	2.457
Ha–Hb		2.386	2.003	1.888	1.867	1.847	1.302	0.866	0.830	0.877
Hc–Hd		2.386	2.064	1.710	1.291	0.910	0.911	0.889	0.914	0.875
Si1–Ru–Si2	87.36(3)	87.9	82.9	81.5	79.7	78.2	80.4	81.8	82.8	81.6
P1–Ru–P2	108.243(17)	98.3	95.3	97.3	95.6	94.1	94.2	93.6	94.0	94.8
Ha–Ru–Hb	89.3(15)	92.1	75.8	70.4	69.6	68.8	46.7	27.9	26.1	28.6
Hb–Ru–Hc	102.5(12)	105.5	73.7	74.8	75.6	77.6	110.1	99.2	81.1	108.4
Hc–Ru–Hd	87.7(15)	92.1	77.3	64.0	47.0	30.8	30.3	29.7	30.9	29.2
Hd–Ru–Ha	176.3(17)	173.0	110.3	97.6	95.9	93.3	81.3	88.6	105.3	79.5
P1–Ru–Ha		87.7	85.5	93.2	89.6	87.9	89.9	92.6	82.9	91.0
P1–Ru–Hb	76.4(10)	78.1	81.5	79.7	81.7	85.1	89.1	93.5	108.9	93.4
P1–Ru–Hc	175.9(11)	176.4	85.4	154.2	156.6	161.7	159.4	154.7	150.8	158.2
P1–Ru–Hd		87.7	162.7	141.3	155.5	166.0	169.1	175.4	171.1	166.4
P2–Ru–Ha		87.7	131.1	147.1	147.4	146.8	131.9	115.7	95.5	114.5
P2–Ru–Hb	175.1(10)	176.4	152.8	81.1	79.4	78.4	85.4	87.8	96.3	85.9
P2–Ru–Hc	72.9(10)	78.1	79.2	82.4	85.8	88.6	94.5	108.6	112.5	85.8
P2–Ru–Hd		87.7	79.9	93.4	92.5	92.5	87.1	81.8	81.9	98.0
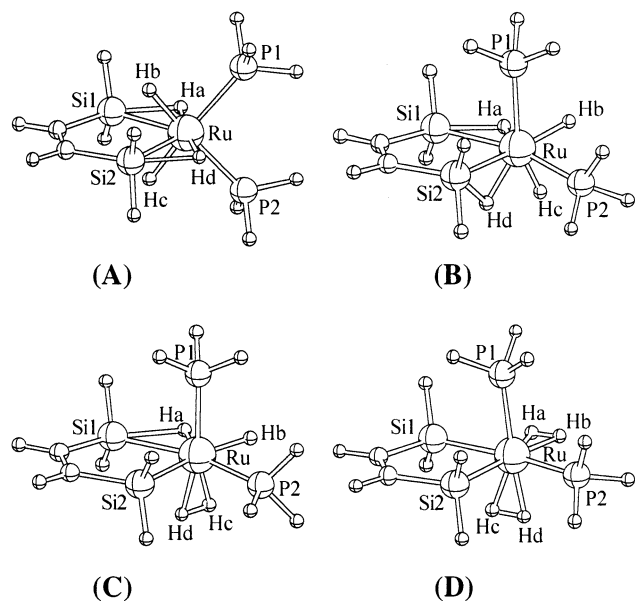
Figure 3. B3LYP-optimized structures for potential RuH$_2$-[(η^2-HSiH$_2$)$_2$(C$_2$H$_2$)](PH$_3$)$_2$ isomers.

sphere. When a C$_6$D$_6$ solution of **2** is pressurized to 3 bar of H$_2$ for 50 min, 10% of **1** is recovered, whereas no formation of **1** was observed after 24 h when using the rigid bis(silane) RuH$_2${(η^2-HSiMe$_2$)$_2$(C$_6$H$_4$)}(PCy$_3$)$_2$ (**3**). However, after bubbling D$_2$ for 20 min into **3**, 30% incorporation of deuterium was observed into the two hydride sites by ^{1}H NMR spectroscopy. The ^{31}P NMR spectrum showed a distortion of the signal at δ 51 characteristic of an isotopic shift.

DFT studies also favor the formation of dihydrogen species. Three other isomers (**B**, **C**, **D**) have been characterized on the singlet potential energy surface (Figure 3) and have been shown to be local minima by vibrational frequency calculations (Table 2). To describe their geometries, the four hydrogen atoms in the

coordination sphere of the metal are labeled a–d. In isomer **A**, the most stable isomer, the two hydrides, denoted Hb and Hc, are *trans* to the phosphines, and their distances from the silicon atoms are only 2.259 Å. We did not locate any dihydrogen analogue Ru(η^2-H$_2$)-[(η^2-HSiH$_2$)$_2$(CH=CH)](PH$_3$)$_2$ of isomer **A**. Isomer **B** has no symmetry and lies 30.9 kJ/mol above **A**. The distances between the hydrides and the silicon atoms are now greater (3.511 and 3.565 Å) than the sum of the van der Waals radii (3.3 Å), whereas the distance between Hc and Hd is 1.710 Å. In isomer **C**, which is 26.3 kJ/mol less stable than **A**, the Si2–Hd bond has been broken, allowing the formation of a dihydrogen ligand Hc–Hd (0.910 Å). The second σ-ligand is the stretched silane Si1–Ha (1.970 Å). The fourth isomer **D**, only 19.9 kJ/mol above **A**, is optimized as a bis-(dihydrogen) complex with H–H distances of 0.866 and 0.889 Å. One of the dihydrogen ligands is located *trans* to the Ru–Si2 bond in the equatorial plane of the pseudo-octahedral structure, and the other one, Hc–Hd, is in axial position, *trans* to the phosphine. Exchange of the four hydrogens can thus occur by rotation of the two dihydrogen ligands. This rotation process may be performed in two different ways: simultaneous rotation of the two dihydrogen ligands or first rotation of Ha–Hb and, in a second step, rotation of Hc–Hd. Rotating both dihydrogen ligands by 90° at the same time produces a characteristic point with two imaginary frequencies (404i and 236i cm^{-1}), requires 19.0 kJ/mol with respect to isomer **D**, and is excluded as a transition state. On the other hand, the rotation of Ha–Hb by 90° corresponds to a transition state **TS$_{rotDab}$** with one imaginary frequency (357i cm^{-1}) and a rotational barrier of 12.4 kJ/mol. In the same way, rotating only Hc–Hd by 90° leads to a transition state **TS$_{rotDcd}$** with one imaginary frequency (249i cm^{-1}) and a rotational barrier of 5.2 kJ/mol. The second pathway, in which rotation of
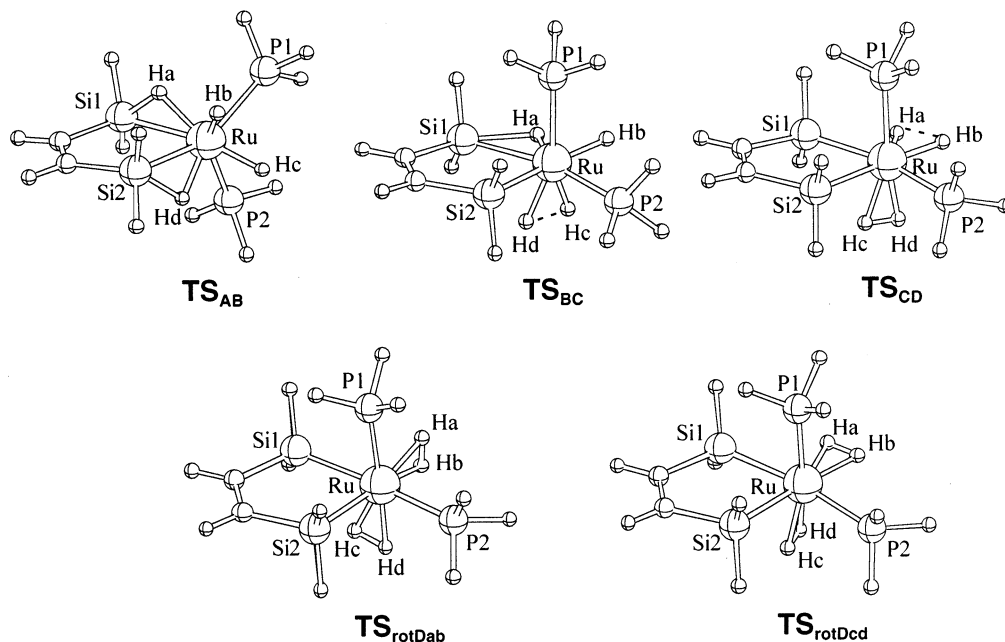
Figure 4. B3LYP-optimized structures of the various transition states involved in the hydrides/(η^2-Si−H) protons exchange process of RuH$_2$[(η^2-HSiH$_2$)$_2$(C$_2$H$_2$)](PH$_3$)$_2$.
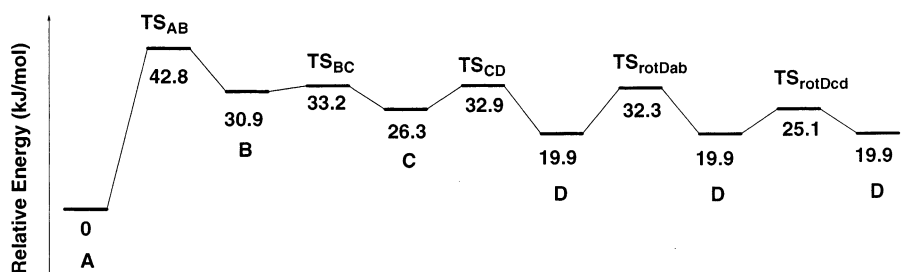

Figure 5. Relative energies (kJ/mol), at the B3LYP level, for the intermediates (see Figure 3) and the transition states (see Figure 4) involved in the hydrides/(η^2-Si−H) protons exchange process of RuH$_2$[(η^2-HSiH$_2$)$_2$(C$_2$H$_2$)](PH$_3$)$_2$. Imaginary vibrational frequencies (cm^{-1}) for the different transition states are 87i (**TSAB**), 519i (**TSBC**), 662i (**TSCD**), 357i (**TSrotDab**), and 249i (**TSrotDcd**).

the dihydrogen ligands occurs sequentially, is thus energetically favored.

All the transition states connecting these four isomers are represented in Figure 4, and selected geometrical parameters are listed in Table 2. A complete picture of the exchange process between the hydrides and the Si−H hydrogens can now be drawn (see Figure 5 and Scheme 2). Conversion of isomer **A** to the asymmetric Ru(η^2-SiH)$_2$ isomer **B** is the prelude to formation of the Ru(η^2-SiH)(η^2-H$_2$) isomer **C** and the Ru(η^2-H$_2$)$_2$ isomer **D**. Exchange occurs via rotation of the dihydrogen ligands and reversal of the isomerization process. It is remarkable that the transformation of **A** into **B** via **TS$_{AB}$** is the most energetically demanding individual step. This corresponds to the breaking of the SISHA interactions between the silicons and the classical hydrides Hb and Hc. The overall barrier to formation of **C** and rotation of the dihydrogen ligands is calculated to be 42.8 kJ/mol.

Mechanism (iii): Generation of a Dangling Si−H Bond. In a third mechanism, first one η^2-SiH bond would be broken by rotation of the Si2 silyl group around the C=C bond. This would result in the formation of a new isomer characterized by three SISHA interactions between Si1 and the hydrides Ha, Hb, and

Hc. This new isomer lies 83.4 kJ/mol above **A** (see Supporting Information). In a subsequent step, the Si1−Ha and Si1−Hb bonds could be broken, allowing the formation of a Ha−Hb ligand as in mechanism (ii). Exchange of the two hydrogens could occur via rotation of the dihydrogen ligand. Thus the value of the exchange barrier calculated for this mechanism is provided by the transition state of the first step. It will be greater than 83.4 kJ/mol, which is not in agreement with the value derived from NMR experiments. Moreover, pathway (iii) is energetically disfavored compared to pathway (ii).

Bis(siloxane) Complex RuH$_2$[(η^2-HSiPh$_2$)$_2$O](P-Cy$_3$)$_2$. The bis(siloxane) complex RuH$_2$\{(η^2-HSiPh$_2$)$_2$O\}-(PCy$_3$)$_2$ (**4**) was isolated from the reaction of **1** with HPh$_2$SiOSiPh$_2$H.[5b] The behavior of **4** when monitored by variable-temperature NMR spectroscopy differed from that of **2** or **3**. A broad line at δ −8.79 was observed for **4** at room temperature in the ^{1}H NMR spectrum (400 MHz, toluene-d_8). A first decoalescence is achieved at 273 K, leading to the appearance at 243 K of two signals of equal intensity, a broad signal at δ −7.77 and a pseudo-triplet at δ −9.57 (J_{H-P} = 45 Hz). A second decoalescence is observed at 213 K, leading at 193 K to five broad signals between δ −7 and δ −10 in a 1:1:1:1:2 integration ratio (Figure 6). The ^{31}P NMR spectrum
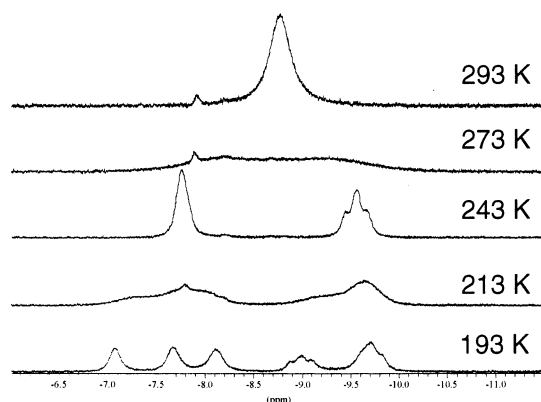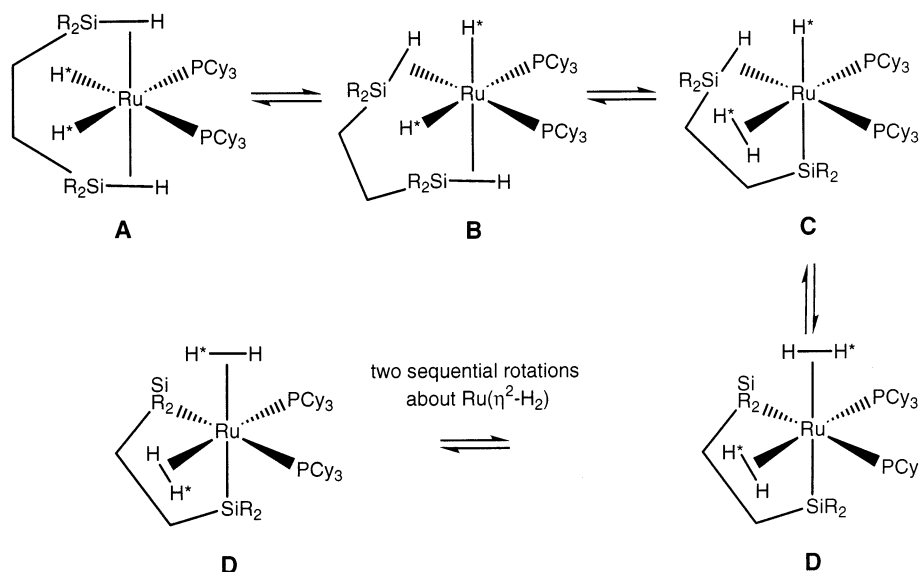
Scheme 2. Exchange Mechanism for 2

Figure 6. Hydride region of the 400 MHz ^{1}H NMR spectra of **4** in C_7D_8 at indicated temperatures.

shows one signal at δ 45.07 at room temperature, which broadens on cooling and finally transforms at 183 K into a singlet at δ 42.4, and an AB pattern at δ 44.9 and 43.1 with J_{P-P} of 28 Hz. A $^{31}P-^1H$ COSY spectrum, acquired at 183 K (Figure 7), helped to assign the spectra. The data are consistent with the existence of two isomers. The symmetrical isomer **4a** is characterized by the singlet in the ^{31}P NMR spectrum and in ^1H NMR spectrum by a broad signal at δ −7.67 for the (η^2-Si−H) protons and a triplet at δ −9.70 for the two hydrides. The asymmetrical isomer **4b** is characterized by the AB pattern indicative of two inequivalent *cis* phosphines and four signals in the ^1H NMR spectrum. In this isomer, all hydrogen atoms in the coordination sphere of the metal are inequivalent: the two broad signals at δ −7.08 and −8.11 are assigned to the two (η^2-Si−H) hydrogens, whereas the two hydrides resonate at δ −8.99 and −9.81, the last signal overlapping the resonance of the hydrides of **4a**. Integration of the signals shows a ratio for **4a**:**4b** of 1:2. The asymmetrical isomer is thus the most thermodynamically stable. For these two isomers, we propose the structures shown in Figure 8. EXSY spectra, recorded at 193 K in toluene-d_8, confirm the exchange between the hydrides and the Si−H hydrogen atoms and also between these two types of hydrogen atoms. However, the isomerization process
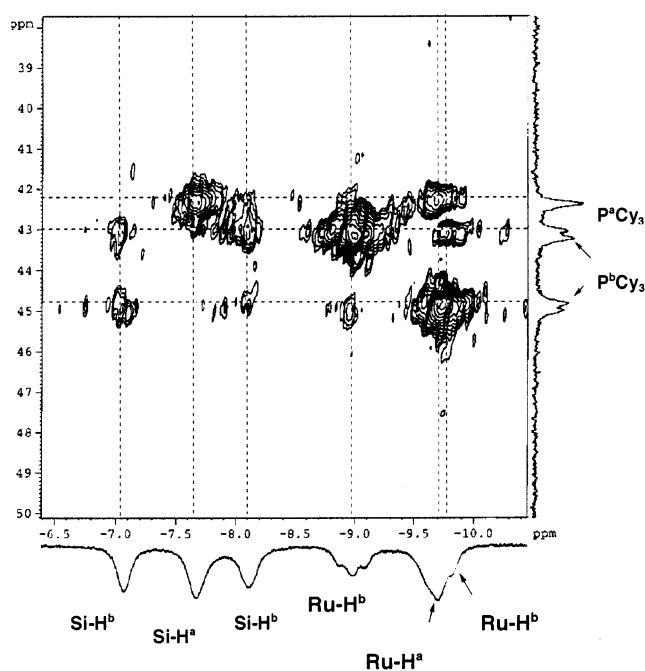

Figure 7. [^{1}H, ^{31}P] HMQC spectrum of **4** in C_7D_8 at 183 K showing both hydride and (η^2-Si−H) proton phosphorus connections for the two isomers (structures shown in Figure 8).
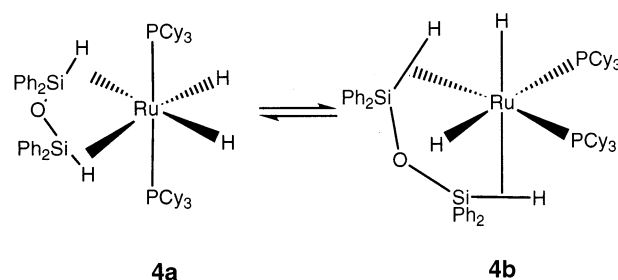

Figure 8. Proposed structures for the two isomers **4a** and **4b**.

between **4a** and **4b** prevents a full analysis. The barrier for exchange between the isomers is lower than the barrier for the exchange between the hydrides and the Si−H hydrogen atoms.
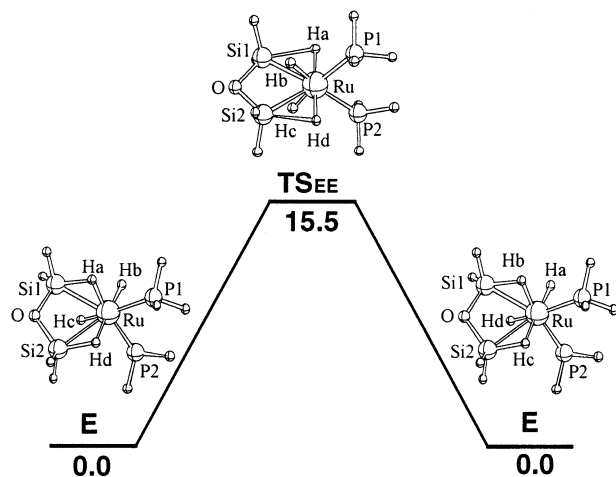
Figure 9. B3LYP-optimized structures and energies for isomer **E** of RuH$_2$[(η^2-HSiH$_2$)$_2$O](PH$_3$)$_2$ and the transition state **TSEE** (243i) involved in the hydrides/(η^2-Si−H) protons exchange process.
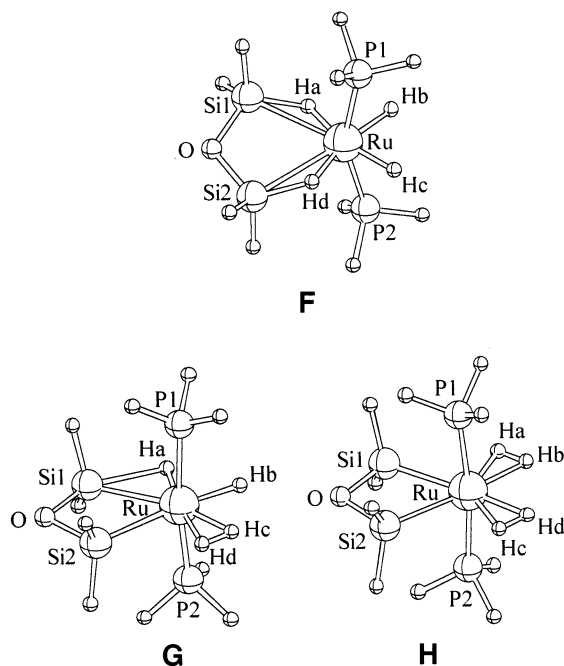

Figure 10. B3LYP-optimized structures for isomers **F**, **G**, and **H**.

It should be noted that when the tetramethyldisiloxane is used in place of the tetraphenyldisiloxane, only the isomer corresponding to **4b** was detected.

A detailed DFT analysis was performed and confirms the existence of two minima **E** (Figure 9) and **F** (Figure 10) corresponding to **4b** and **4a**, respectively. The calculated geometrical parameters are listed in Table 3. Isomer **E** has no symmetry. The phosphines are in a *cis* position, but there are different substituents in the mutually *trans* sites, i.e., a hydride and a Si−H ligand. Moreover, the extents of activation of the two Si−H bonds are different (1.784 and 1.596 Å), and consequently, the Si$\cdots$H distances are also very different (Si1$\cdots$Hc = 2.125 Å, Si2$\cdots$Hb = 4.181 Å, Si1$\cdots$Hb = 2.913 Å, Si2$\cdots$Hc = 2.670 Å). This geometry contrasts with the results obtained for **2** and other bis(silane) complexes with two or more atoms bridging the two silicon atoms. In these cases, a symmetrical arrange-

Table 3. Selected Geometrical Parameters for the Isomer E and the Transition State TS$_{EE}$

	E	TS$_{EE}$
Si1−Ha	1.784	2.062
Si1−Hb	2.913	2.216
Si2−Hc	2.670	2.216
Si2−Hd	1.596	2.062
Ru−Ha	1.658	1.690
Ru−Hb	1.614	1.624
Ru−Hc	1.627	1.624
Ru−Hd	1.805	1.690
Ru−Si1	2.442	2.405
Ru−Si2	2.700	2.405
Si1−O	1.687	1.689
Si2−O	1.658	1.689
Si1−Ru−Si2	65.2	67.4
Si1−O−Si2	112.3	104.4
P1−Ru−P2	96.1	97.3
Ha−Ru−Hb	86.5	90.6
Hb−Ru−Hc	82.9	114.6
Hc−Ru−Hd	102.8	90.6
Hd−Ru−Ha	92.4	178.0
Si1−Ha−Ru	90.3	79.0
Si1−Hb−Ru	57.0	75.8
Si2−Hc−Ru	73.4	75.8
Si2−Hd−Ru	105.0	79.0
P1−Ru−Ha	79.1	89.3
P1−Ru−Hb	85.0	74.1
P1−Ru−Hc	166.9	171.4
P1−Ru−Hd	89.3	89.3
P2−Ru−Ha	170.5	89.3
P2−Ru−Hb	84.9	171.4
P2−Ru−Hc	77.9	74.1
P2−Ru−Hd	95.8	89.3

ment is observed by X-ray and DFT data, with equivalent Si−H and Si$\cdots$H distances. Unfortunately, it was not possible to obtain crystals of **4** suitable for an X-ray analysis. The calculated geometry **E** resembles the geometry of **B**, the unstable isomer of **2**. In isomer **E**, the exchange between the hydrides and the (η^2-Si−H) hydrogen atoms occurs readily via a transition state **TS$_{EE}$** only 15.5 kJ/mol above **E**. **TS$_{EE}$** has a C_{2v} geometry, resulting in a *trans* position of the (η^2-Si−H) hydrogen atoms (the Hd−Ru−Ha angle is 178.0°). The four Si$\cdots$H distances are now almost equivalent (2.062 and 2.216 Å) and correspond to SISHA interactions (Table 3). Isomer **F** is only 9.3 kJ/mol above **E**. This difference in energy is small enough that, in this specific case, a change in the relative energies of **E** and **F** cannot be excluded if PCy$_3$ were used in place of PH$_3$ as a model. **F** is characterized by the coordination of a disiloxane ligand in an early stage of activation (Si−H = 1.609 Å) with no SISHA interactions (Si$\cdots$H 3.527 Å). The two phosphines are pushed away from the disiloxane to avoid steric repulsion (P−Ru−P angle = 157.5°) (Table 4). Two other isomers (**G**, **H**) have been characterized on the singlet potential energy surface (Figure 10). Vibrational frequency calculations show them as local minima. In isomer **G**, which is 16 kJ/mol less stable than **F**, the Si2−Hd bond is extremely stretched, allowing the formation of a dihydrogen ligand Hc−Hd (0.866 Å). The second silane Si1−Ha is also stretched (2.006 Å). The second isomer **H**, only 5.1 kJ/mol above **F**, is optimized as a bis(dihydrogen) complex with H−H distances of 0.863 Å. All the transition states connecting these three isomers are represented in Figure 11, and their geometrical parameters are listed in Table 4. The energetics of the exchange pathway between the hydrides and the Si−H hydrogens are illustrated in Figure

Table 4. Selected Geometrical Parameters for the Isomers F−H and the Corresponding Transition States

	F	TS$_{FG}$	G	TS$_{GH}$	H	TS$_{rotH}$
Si1−Ha	1.609	1.769	2.006	2.404	2.823	3.227
Si1−Hb	3.527	3.650	3.704	3.534	3.505	3.227
Si2−Hc	3.527	3.259	3.310	2.779	3.505	2.880
Si2−Hd	1.609	2.170	2.586	3.457	2.823	3.552
Ru−Ha	1.742	1.682	1.622	1.621	1.784	1.826
Ru−Hb	1.622	1.656	1.622	1.665	1.817	1.826
Ru−Hc	1.622	1.652	1.775	1.821	1.817	1.781
Ru−Hd	1.742	1.653	1.796	1.813	1.784	1.825
Ru−Si1	2.666	2.539	2.449	2.430	2.437	2.435
Ru−Si2	2.666	2.500	2.511	2.501	2.437	2.429
Ha−Hb	2.081	2.043	1.953	1.351	0.863	0.834
Hc−Hd	2.081	1.201	0.866	0.852	0.863	0.861
Si1−Ru−Si2	62.6	61.2	61.2	62.8	64.5	65.2
Si1−O−Si2	112.1	99.1	96.6	99.0	100.5	101.3
P1−Ru−P2	157.5	167.3	171.2	177.0	174.1	170.3
Ha−Ru−Hb	76.3	75.5	73.0	48.5	27.7	26.4
Hb−Ru−Hc	83.3	77.9	71.6	100.8	75.3	111.8
Hc−Ru−Hd	76.3	42.6	28.1	27.1	27.7	27.6
Hd−Ru−Ha	124.5	164.1	172.6	122.2	130.7	85.0
Si1−Ha−Ru	105.3	94.7	84.2	71.3	58.8	48.5
Si1−Hb−Ru	45.9	37.3	31.6	37.4	40.8	48.5
Si2−Hc−Ru	45.9	48.7	48.4	61.8	40.8	57.2
Si2−Hd−Ru	105.3	80.4	67.1	44.2	58.8	39.2
P1−Ru−Ha	100.8	89.2	87.0	88.8	91.2	80.0
P1−Ru−Hb	81.5	83.7	86.0	89.9	92.3	106.3
P1−Ru−Hc	81.7	87.9	90.5	91.3	92.3	92.2
P1−Ru−Hd	89.7	92.5	92.2	91.6	91.2	94.0
P2−Ru−Ha	89.7	89.2	87.4	88.8	91.2	106.3
P2−Ru−Hb	81.7	83.7	85.9	89.9	92.3	80.0
P2−Ru−Hc	81.5	87.9	90.2	91.7	92.3	92.2
P2−Ru−Hd	100.8	92.5	92.5	91.3	91.2	94.0

TS$_{FG}$ **TS$_{GH}$**

TS$_{rotH}$
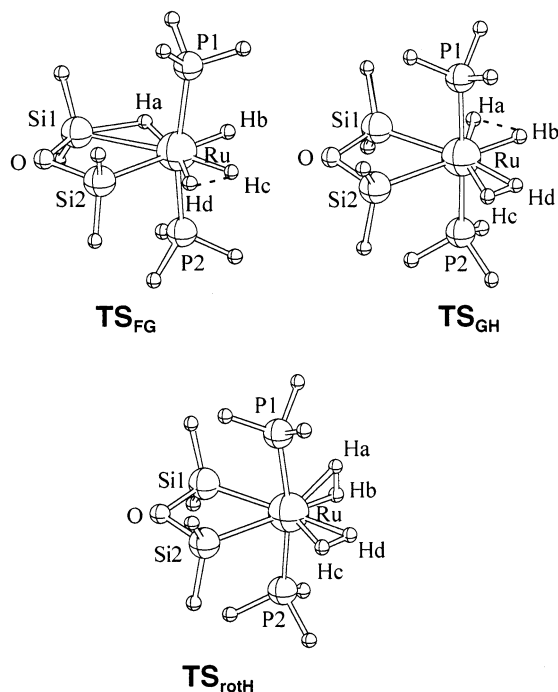
Figure 11. B3LYP-optimized structures for the transition states derived from **F** and involved in the hydrides/(η^2-Si−H) protons exchange process.

12. The symmetric (η^2-SiH)$_2$ isomer **F** is converted to the (η^2-SiH)(η^2-H$_2$) species **G** and the (η^2-H$_2$)$_2$ isomer **H**. Internal rotation of the dihydrogen ligands and reversal of the isomer interconversion processes complete the exchange (Scheme 3).

It is remarkable that in all these processes two different σ-bonds, σ-H−H and σ-H−Si, compete for the
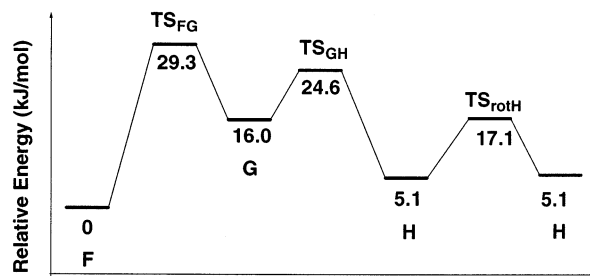
Figure 12. Relative energies (kJ/mol) at the B3LYP level for the intermediates (Figure 10) and the transition states (Figure 11) involved in the hydrides/(η^2-Si−H) protons exchange process of RuH$_2$[(η^2-HSiH$_2$)$_2$O](PH$_3$)$_2$. Imaginary vibrational frequencies (cm^{-1}) for the different transition states are 841i (**TSFG**), 707i (**TSGH**), and 390i (**TSrotH**).

Scheme 3.   Exchange Mechanism for 4

(F)   (G)

two sequential
rotations
about Ru(η^2-H$_2$)

(H)   (H)
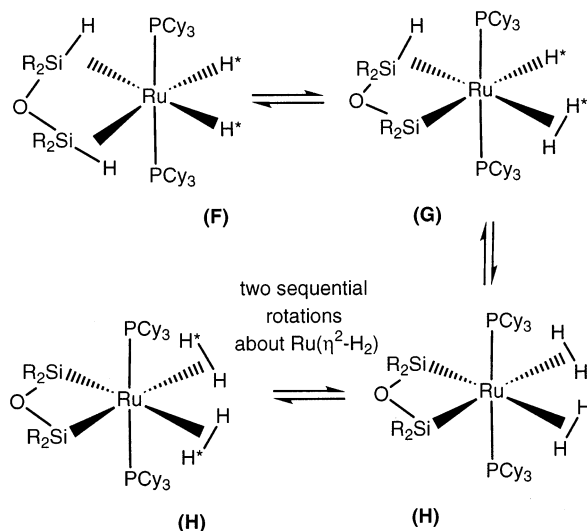
stabilization of various intermediates. As soon as one σ-bond is stretched, another one will be formed.

Reactivity of 4 with PPh$_3$. We have previously shown that substitution of one or two PCy$_3$ by PR$_3$ (R = Ph, pyl with pyl = pyrollyl) in the bis(silane) complexes RuH$_2${(H-SiR$_2$)$_2$X}(PCy$_3$)$_2$ (X = C$_6$H$_4$, (CH$_2$)$_2$, (CH$_2$)$_3$, OSiMe$_2$O) results in the formation of the corresponding mono- or bis(phosphine) complexes RuH$_2${(H-SiR$_2$)$_2$X}(PCy$_3$)$_{2-n}$(PR$_3$)$_n$. In the case of **4**, the disiloxane is much more labile. This is illustrated by its ready elimination from **4** upon addition of 1 or 2 equiv of Ppyl$_3$, with formation of RuH$_2$(H$_2$)(Ppyl$_3$)(PCy$_3$)$_2$ or RuH$_2$-(Ppyl$_3$)$_4$, respectively.[5b] However, by using an excess of triphenylphosphine (5 equiv), we were able to isolate a new compound, **5**, formulated as RuH$_2${(η^2-H-SiPh$_2$)O-(SiHPh$_2$)}(PPh$_3$)$_3$ (Scheme 4). The NMR data are consistent with a disiloxane ligand coordinated to the ruthenium with only one Si−H bond. The ^{1}H NMR spectrum (400 MHz, toluene-d_8) at room temperature shows a second-order signal at δ −9.12 for the three hydrogens bound to the ruthenium which are in rapid exchange. The dangling Si−H proton resonates as a sharp singlet at δ 5.31 ($^1J_{Si-H}$ = 220 Hz). The ^{1}H{^{31}P} NMR spectrum in thf-d_8 allows the measurement of an apparent J_{Si-H} constant of 34 Hz for the high-field signal. At room temperature the ^{31}P NMR spectrum shows one singlet at δ 40.14. The ^{1}H and ^{31}P NMR spectra are temperature dependent. At 213 K, two broad

Scheme 4

X = H, (**5**); OH, (**6**)
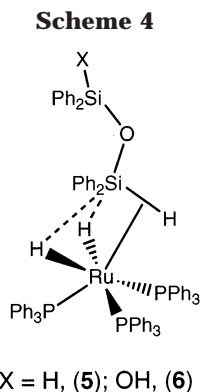
multiplets are observed in the ^{1}H NMR spectrum at δ −8.75 and −9.15 ($J_{\text{H–Pcis}}$ = 25 Hz and $J_{\text{H–Ptrans}}$ = 50 Hz) in a 2:1 integration ratio (Figure 13). At this temperature, the ^{31}P NMR spectrum displays a triplet at δ 42.62 and a doublet at δ 38.49 with $J_{\text{P–P}}$ of 23 Hz. The ^{29}Si–^{1}H COSY spectrum acquired at 203 K shows two Si signals at δ 28, correlating with the low-field signal of the dangling Si–H, and a singlet at δ 10, which correlates to the high-field signal at δ −9.1 attributed to the (η^2-Si–H) hydrogen. The ^{31}P–^{1}H COSY spectrum confirms the presence of two hydrides at 203 K that correlate with the ^{31}P resonances.
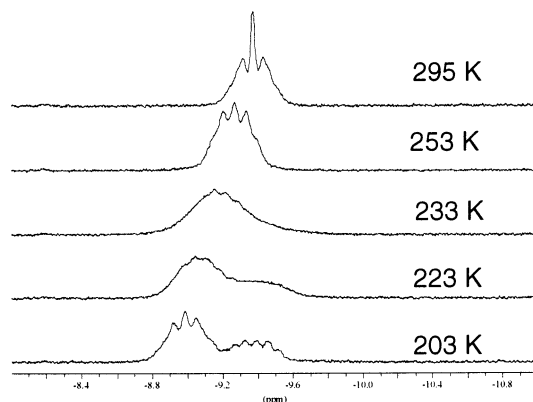

Figure 13. Hydride region of the 400 MHz ^{1}H NMR spectra of **5** in C$_7$D$_8$ at indicated temperatures.

Attempts to obtain crystals of **5** suitable for an X-ray determination failed, but crystals of the partially hydrolyzed complex RuH$_2$\{(η^2-H-SiPh$_2$)O(Si(OH)Ph$_2$)\}-(PPh$_3$)$_3$ (**6**) were obtained (Scheme 4). This complex exhibits essentially the same NMR spectra apart from the absence of the ^{1}H NMR signal corresponding to the dangling Si–H now transformed into a Si–OH group. The X-ray structure determined at 140 K is shown in Figure 14 (see Table 5). The ruthenium is surrounded by three phosphines in a tripodal position with P–Ru–P angles of 103° (av) and Si–Ru–P angles of 115.0° (av). The Ru–Si(1) distance is 2.3539(15) Å, thus at the lower limit of the Ru–Si distances observed in other silyl ruthenium complexes. The second silicon atom is far away from the ruthenium. Due to the quality of the data, analysis of the distances involving the hydrogen atoms bound to the ruthenium should be considered cautiously. Three hydrogen atoms were, however, located in the vicinity of the ruthenium with Ru–H distances of 1.6 Å (av). The distances between the silicon and these three hydrogens are 1.97(5), 2.03(5), and 2.07(5) Å.
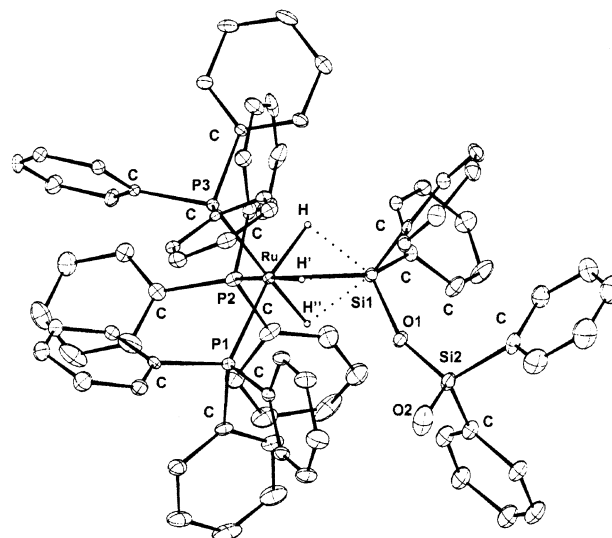

Figure 14. CAMERON drawing of RuH$_2$\{(H-SiPh$_2$)O(Si-(OH)Ph$_2$)\}(PPh$_3$)$_3$ (**6**). Selected bond lengths (Å): Ru–Si-(1), 2.3539 (15); Ru–P(1), 2.3618 (13); Ru–P(2), 2.4234 (14); Ru–P(3), 2.4154 (13); Ru–H, 1.59 (3); Ru–H′, 1.61 (5); Ru–H″, 1.57 (3); Si(1)–H, 1.97 (5); Si(1)–H′, 2.03 (5); Si(1)–H″, 2.07 (5). Selected bond angles (deg): P(1)–Ru–P(2), 102.75 (5); P(1)–Ru–P(3), 100.46 (4); P(3)–Ru–P(2), 106.72 (5); Si(1)–Ru–P(1), 113.04 (5); Si(1)–Ru–P(2), 113.41 (5); Si(1)–Ru–P(3), 118.60 (5).

Table 5. Crystal Data for RuH$_2$\{(H-SiPh$_2$)O(Si(OH)Ph$_2$)\}(PPh$_3$)$_3$ (6)

chemical formula	C$_{78}$H$_{69}$O$_2$P$_3$RuSi$_2$, 1/4(C$_4$H$_9$O, C$_2$H$_6$O)
fw	1319.75
cryst syst	monoclinic
space group	$C2/c$
Z, calcd density, Mg/m^3	8, 1.233
abs coeff, mm^{-1}	0.370
$F(000)$	5460
a, Å	40.246 (3)
b, Å	19.777 (3)
c, Å	17.734 (4)
β, deg	91.03 (2)
V, Å	14113 (4)
temp, K	140 (2)
no. of data/restraints/params	9282/196/902
goodness of fit on F^2	0.996
R1 [$I>2\sigma(I)$]	0.0485
wR2	0.1119
largest diff peak and hole, e/Å^{-3}	1.063 and −0.403

A few ruthenium complexes of general formula RuH$_3$-(SiR$_3$)(PR$_3$)$_3$ have been reported as well as osmium and iron analogues.[16−19] The nature of the metal–silicon bond and of the Ru···H···Si interactions has been discussed specifically. Very recently the X-ray structure of RuH$_3$(SiCl$_2$Me)(PPh$_3$)$_3$ has been reported, and the

(16) Yardy, N. M.; Lemke, F. R.; Brammer, L. *Organometallics* **2001**, *20*, 5670.

(17) (a) Kono, H.; Wakao, N.; Ito, K.; Nagai, Y. *J. Organomet. Chem.* **1977**, *132*, 53. (b) Haszeldine, R. N.; Malkin, L. S.; Parish, R. V. *J. Organomet. Chem.* **1979**, *182*, 323. (c) Procopio, L. J.; Berry, D. H. *J. Am. Chem. Soc.* **1991**, *113*, 4039. (d) Gilbert, S.; Knorr, M.; Mock, S.; Schubert, U. *J. Organomet. Chem.* **1994**, *480*, 241.

(18) (a) Rickard, C. E. F.; Roper, W. R.; Woodgate, S. D.; Wright, L. J. *J. Organomet. Chem.* **2000**, *609*, 177. (b) Mohlen, M.; Rickard, C. E. F.; Roper, W. R.; Salter, D. M.; Wright, L. J. *J. Organomet. Chem.* **2000**, *593–594*, 458.

(19) (a) Hubler, K.; Hubler, U.; Roper, W. R.; Schwerdtfeger, P.; Wright, L. J. *Chem. Eur. J.* **1997**, *3*, 1608. (b) Buil, M.; Espinet, P.; Esteruelas, M. A.; Lahoz, F. J.; Lledós, A.; Martinez-Ilarduya, J. M.; Maseras, F.; Modrego, J.; Oñate, E.; Oro, L. A.; Sola, E.; Valero, C. *Inorg. Chem.* **1996**, *35*, 1250.

three hydrogens have been located.[16] Three Si···H distances of 1.86(2), 1.94(2), and 1.94(3) Å were reported. The complex was formulated, on the basis of the X-ray and NMR data, as a trihydridosilyl species with Ru−H···Si interactions consistent with interligand hypervalent interaction theory (IHI).[20] The hydrides and the phosphines were found to be equivalent, but it seems that NMR data were acquired in a rather narrow range (223−298 K). Similar data were reported for the osmium complex $OsH_3(Si\{OCH_2CH_2\}_3N)(PPh_3)_3$.[18a]

In the present system, it is notable that decoalescence was achieved for **5** near 233 K (see above). We thus favor a dihydride(σ-silane) formulation for **5** (Scheme 4) with SISHA interactions between the silicon and two hydrides $RuH_2\{(\eta^2-H-SiPh_2)O(SiHPh_2)\}(PPh_3)_3$. We have previously described the properties of a similar dihydride(σ-silane) complex, $RuH_2(\eta^2-H_2)(\eta^2-H-SiPh_3)(PCy_3)_2$, in which the dihydrogen ligand plays the role of the phosphine in **5**.[6] This complex exhibited Si···H distances by X-ray (and DFT) of 1.72(3) (1.946), 1.83(3) (2.071), and 2.40(4) Å (2.116 Å), also consistent with the presence of an (η^2-Si−H) bond and two hydrides with SISHA interactions.
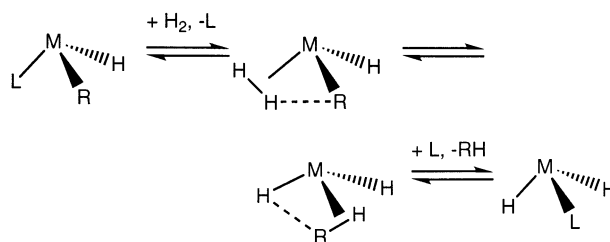
The work of Nikonov has highlighted the existence of secondary interactions between halosilyl ligands and hydrides.[20] In our systems, we have demonstrated that SISHA interactions occur in the absence of electron-withdrawing substituents. Further analysis of the relation between the two types of interactions will be published elsewhere.

Conclusion

The bis(silane) complexes of general formula $RuH_2\{(\eta^2-H-SiR_2)_2X\}(PR_3)_2$ are stabilized by two σ-Si−H bonds and by nonbonding H−Si···H interactions. The present study highlights the importance of these "weak" interactions, denoted SISHA interactions. They play a dramatic role in the exchange process between the two types of hydrogen, as their breaking is responsible for the most energetically demanding step. They allow smooth variations leading to the formation of new σ-bonds (in this case dihydrogen ligands) without the necessity of decoordination of a ligand. Two mechanisms are commonly proposed for conversion of a complex M(H)X to MH(Y) by reaction with HY (X, Y = H alkyl, aryl, silyl, etc): σ-bond metathesis and reductive elimination/oxidative addition.[1,21] The σ-ligand substitution mechanism proposed in this paper offers a third alternative to this important class of reactions which could be of considerable importance in catalytic reactions (Scheme 5). It can be related to a mechanism recently proposed in the field of alkane dehydrogenation. An interchange process is proposed to occur through an RH/H$_2$ exchange transition state on iridium(III) complexes, keeping the oxidation state constant.[22]

A comparison can be made between these SISHA interactions and the familiar phenomenon of hydrogen

Scheme 5. σ-Ligand Susbtitution Mechanism

bonding with its tremendous influence in biology and chemistry.[23] Dihydrogen bonds have recently been recognized as a special class of secondary bond which may influence reactivity and structure.[24] Intramolecular dihydrogen bonds may result from an interaction between a hydride and a hydrogen atom of another ligand, while intermolecular dihydrogen bonds may form between a hydride and, for example, a hydrogen from an alcohol.[24] All these interactions display the same order of bond energies (up to 40 kJ/mol), but the H···H and Si···H distances are necessarily different: 1.7−1.9 Å (sum of the van der Waals radii of two H atoms: 2.4 Å) versus 2.0−2.5 Å (sum of the van der Waals radii of H and Si atoms: 3.3 Å). The studies reported here contribute to our understanding of the importance of "weak" interactions. There is clearly still much to learn about the role of any "weak" interactions in catalysis.

Experimental Section

General Considerations. All reactions were carried out under an argon atmosphere using standard Schlenk techniques. Solvents were dried and distilled according to standard procedures and degassed prior to use. All reagents were purchased from Aldrich except $RuCl_3 \cdot 3H_2O$, which came from Johnson Matthey Ltd, and were used without further purification. The following chemicals were prepared according to published procedures: $RuH_2(H_2)_2(PCy_3)_2$,[25] $RuH_2[(\eta^2-HSiMe_2)-(CH_2)_2](PCy_3)_2$,[5b] $RuH_2[(\eta^2-HSiMe_2)_2O](PCy_3)_2$,[5b] $RuH_2[(\eta^2-HSiPh_2)_2O](PCy_3)_2$.[5b] All NMR solvents were dried using appropriate methods and degassed prior to use. The NMR measurements were made using NMR tubes fitted with J. Young Teflon valves, and solvents were added by vacuum transfer on a high-vacuum line. NMR spectra were recorded on Bruker AC 200 or DRX-400 spectrometer with ^1H at 400.13 or 200.13 and ^{31}P at 161.9 or 80.95 MHz, respectively. ^1H NMR chemical shifts are reported in ppm relative to residual ^1H signals in toluene-d_7, δ 2.13, and ^{31}P NMR in ppm downfield of an external 85% solution of phosphoric acid. Temperatures were calibrated via a methanol chemical shift thermometer. Standard COSY,[26] HMQC,[27] and EXSY[28] (1D and 2D pulse sequences) were used as previously described. In a typical EXSY run, data were collected at selected temperatures for a series of mixing times τ (e.g., 25, 50, 75, 100, 200, 400, and 600 ms). The sum of the integrals of the diagonal peak areas

(20) (a) Nikonov, G. I.; Kuzmina, L. G.; Vyboishchikov, S. F.; Lemenovskii, D. A.; Howard, J. A. K. *Chem. Eur. J.* **1999**, *5*, 2947. (b) Nikonov, G. I.; Mountford, P.; Green, J. C.; Cooke, P. A.; Leech, M. A.; Blake, A. J.; Howard, J. A. K.; Lemenovskii, D. A. *Eur. J. Inorg. Chem.* **2000**, 1917. (c) Nikonov, G. I. *J. Organomet. Chem.* **2001**, *635*, 24.
(21) Tilley, T. D. *Acc. Chem. Res.* **1993**, *26*, 22.
(22) Haenel, M. W.; Oevers, S.; Angermund, K.; Kaska, W. C.; Fan, H.-J.; Hall, M. B. *Angew. Chem., Int. Ed.* **2001**, *40*, 3596.

(23) Jeffrey, G. A.; Saenger, W. In *Hydrogen Bonding in Biological Structures*; Springer: Berlin, 1994.
(24) Custelcean, R.; Jackson, J. E. *Chem. Rev.* **2001**, *101*, 1963.
(25) Borowski, A. F.; Sabo-Etienne, S.; Christ, M. L.; Donnadieu, B.; Chaudret, B. *Organometallics* **1996**, *15*, 1427.
(26) (a) Aue, W. P.; Bartholdi, E.; Ernst, R. R. *J. Chem. Phys.* **1976**, *64*, 2229. (b) Nagayama, K.; Kumar, A.; Wuthrich, K.; Ernst, R. R. *J. Magn. Reson.* **1980**, *40*, 321.
(27) (a) Sorensen, O. W.; Eich, G. W.; Levitt, M. H.; Bodenhausen, G.; Ernst, R. R. *Progress in NMR Spectrosc.* **1983**, *16*, 163. (b) Wagner, G.; Bodenhasuen, G.; Muller, N.; Rance, M.; Sorensen, O. W.; Ernst, R. R.; Wuthrich, K. *J. Am. Chem. Soc.* **1985**, *107*, 6440.
(28) (a) Kessler, H.; Gehrke, M.; Griesinger, C. *Angew. Chem., Int. Ed. Engl.* **1988**, *27*, 490. (b) Stott, K.; Stonehouse, J.; Keeler, J.; Hwang, T. L.; Shaka, A. J. *J. Am. Chem. Soc.* **1995**, *117*, 4199.

for a given hydride location and the cross-peak areas arising from exchange were normalized to 100%. For processes such as this, involving the exchange of nuclei between two sites, exact rate constants can then be determined via analysis of the intensity versus mixing time profile or via the more comprehensive matrix method.[14] The experiment was repeated over a range of temperatures, and the activation parameters $\Delta H^{\ddagger}$ and $\Delta S^{\ddagger}$ were determined by nonlinear regression using SPSS for Windows version 9.0.

Synthesis and Characterization of RuH₂{(η²-H-SiPh₂)O-(SiHPh₂)}(PPh₃)₃ (5). A solution of triphenylphosphine (313 mg, 1.20 mmol) and RuH₂[(η²-HSiPh₂)₂O](PCy₃)₂ (**4**) (250 mg, 0.24 mmol) in pentane (15 mL) was stirred overnight at room temperature. The resulting white powder was filtered off and washed with small amounts of pentane before being dried under argon and finally under vacuum (yield 85%). Anal. Calcd for $C_{78}H_{68}OSi_2P_3Ru$: C, 73.71; H, 5.35. Found: C, 74.13; H, 5.71. ¹H NMR (toluene-*d₈*, 400.13 MHz) 293 K: δ 9.12 (m, 3H, RuH₃), 5.31 (s, 1H, Si−H), 6.9−7.9 (m, 45H, PPh₃); 213 K: −8.75 (brt, 2H, RuH₃), −9.15 (dt, 1H, RuH₃), 5.26 (s, 1H, Si−H). ³¹P{¹H} NMR (toluene-*d₈*, 161.97 MHz) 293 K: 40.14 (s); 213 K: 42.62 (t, J_{P-P} = 23 Hz), 38.49 (d, J_{P-P} = 23 Hz). ¹H NMR (thf-*d₈*, 500.13 MHz) 300 K: −9.65 (m, 3H, RuH₃), 4.61 (s, 1H, Si−H), 6.8−7.4 (m, 45H, PPh₃); 203 K: −9.73 (t, 1H, RuH₃), −9.43 (dt, 2H, RuH₃), 4.23 (s, 1H, Si−H). ³¹P{¹H} NMR (thf-*d₈*, 202.46 MHz, 300 K): 39.62 (s). ¹H−²⁹Si{¹H} INEPT (C₆D₆, 293 K, 79.5 MHz): −21.4 (s, Si−H), 11.69 (d, J_{Si-P} = 9.4 Hz, Ru−H−Si).

Synthesis and Characterization of RuH₂{(η²-H-SiPh₂)O-[Si(OH)Ph₂]}(PPh₃)₃ (6). Several attempts were made to obtain crystals of **5** suitable for an X-ray determination. They were all unsuccessful. However, slow diffusion of pentane into a THF solution of **5** resulted, after several days, in a few yellow crystals characterized by NMR and X-ray structure as RuH₂-{(η²-H-SiPh₂)O[Si(OH)Ph₂]}(PPh₃)₃ (**6**). **6** derives from **5** probably as a result of partial hydrolysis due to water contamination. ¹H NMR (toluene-*d₈*, 400.13 MHz, 293 K): δ −9.15 (m, 3H, RuH₃), 6.9−7.9 (m, 45H, PPh₃).

Crystal Data for 6. Data were collected at low temperature (Table 5) on a Stoe imaging plate diffraction system (IPDS), equipped with an Oxford Cryosystems cryostream cooler device and using graphite-monochromated Mo Kα radiation (λ = 0.71073 Å). A half-sphere of data was collected by φ axis rotation with an increment of 1.5° over 200° and 133 exposures. The final unit cell parameters were obtained by least-squares refinement of a set of 5000 well-measured reflections, and crystal decay was monitored by measuring 200 reflections by image. No significant fluctuation of the intensities was observed. The structure was solved by direct methods using the program SIR92[29] and refined by least-squares procedures on F^2 with SHELXL-93.[30] The atomic scattering factors were taken from International Tables for X-Ray Crystallography.[31] All hydrogen atoms were located on a difference Fourier map, but introduced and refined with a riding model. Hydride atoms labeled H, H′, and H″ were isotropically refined by using a free variable for the U[iso]. All non-hydrogen atoms were anisotropically refined, and a weighting scheme was used in the last cycles of refinement. Weights are calculated from the

following formula: $w = 1/[\sigma^2(F_o^2) + (aP)^2 + bP]$ where $P = (F_o^2 + 2F_c^2)/3$. Statistical disorder was observed on some phenyl rings. A model was found in each case and refined by using some restraints on interatomic lengths and angles and on some anisotropic displacement parameters in order to lead to reasonable chemical models. Two distinct solvent molecules were also located: tetrahydrofuran and ethanol. The best convergence was obtained with occupancy values equal to 0.25. Some restraints on interatomic distances, angles, and anisotropic displacement parameters were necessary to improve the models. The molecule was drawn with the program CAMERON with 40% probability displacement ellipsoids for non-hydrogen atoms.[32]

Theoretical Methods

DFT calculations were performed with the Gaussian 98 series of programs[33] using the nonlocal hybrid functional denoted as B3LYP.[34] For ruthenium, the core electrons were represented by a relativistic small-core pseudopotential using the Durand−Barthelat method.[35] The 16 electrons corresponding to the 4s, 4p, 4d, and 5s atomic orbitals were described by a (7s, 6p, 6d) primitive set of Gaussian functions contracted to [5s, 5p, 3d]. Standard pseudopotentials developed in Toulouse were used to describe the atomic cores of all other non-hydrogen atoms (C, O, Si, and P).[36] A double plus polarization valence basis set was employed for each atom (d-type function exponents were 0.80 and 0.85, 0.45 and 0.45, respectively). For hydrogen, a standard primitive (4s) basis contracted to [2s] was used. A p-type polarization function was added for the hydrogen atoms directly bound to ruthenium. The geometry of the various critical points on the potential energy surface was fully optimized with the gradient method available in Gaussian 98. Calculations of harmonic vibrational frequencies were performed to determine the nature of each critical point.

Supporting Information Available: Tables and figures of more extensive computational results. X-ray crystallographic files (CIF). This material is available free of charge via the Internet at http://pubs.acs.org.

OM0206148

(29) Sheldrick, G. M. *SHELXL-93*, Program for Crystal Structure Refinement; Göttingen: Germany, 1993.

(30) Altomare, A.; Cascarano, G.; Giacovazzo, G.; Guagliardi, A.; Burla, M. C.; Polidori, G.; Camalli, M. *J. Appl. Crystallogr.* **1994**, *27*, 435.

(31) *International Tables for X-ray Crystallography*; Kynoch Press: Birmingham, England, 1974; Vol IV.

(32) Watkin, D. M.; Pearce, L.; Prout, C. K. *CAMERON*−A Molecular Graphics Package; Chemical Crystallography Laboratory, University of Oxford, 1993.

(33) Frisch, M. J.; Trucks, G. W.; Schlegel, H. B.; Scuseria, G. E.; Robb, M. A.; Cheeseman, J. R.; Zakrzewski, V. G.; Montgomery, J. A., Jr.; Stratmann, R. E.; Burant, J. C.; Dapprich, S.; Millam, J. M.; Daniels, A. D.; Kudin, K. N.; Strain, M. C.; Farkas, O.; Tomasi, J.; Barone, V.; Cossi, M.; Cammi, R.; Mennucci, B.; Pomelli, C.; Adamo, C.; Clifford, S.; Ochterski, J.; Petersson, G. A.; Ayala, P. Y.; Cui, Q.; Morokuma, K.; Malick, D. K.; Rabuck, A. D.; Raghavachari, K.; Foresman, J. B.; Cioslowski, J.; Ortiz, J. V.; Stefanov, B. B.; Liu, G.; Liashenko, A.; Piskorz, P.; Komaromi, I.; Gomperts, R.; Martin, R. L.; Fox, D. J.; Keith, T.; Al-Laham, M. A.; Peng, C. Y.; Nanayakkara, A.; González, C.; Challacombe, M.; Gill, P. M. W.; Johnson, B.; Chen, W.; Wong, M. W.; Andrés, J. L.; Gonzalez, C.; Head-Gordon, M.; Replogle, E. S.; Pople, J. A. *Gaussian 98*, Revision A.6; Gaussian, Inc.: Pittsburgh, PA, 1998.

(34) (a) Becke, A. D. *J. Chem. Phys.* **1993**, *98*, 5648. (b) Lee, C.; Yang, W.; Parr, R. G. *Phys. Rev. B* **1988**, *37*, 785.

(35) Durand, P.; Barthelat, J.-C. *Theor. Chim. Acta* **1975**, *38*, 283.

(36) Bouteiller, Y.; Mijoule, C.; Nizam, M.; Barthelat, J.-C.; Daudey, J. P.; Pélissier, M.; Silvi, B. *Mol. Phys.* **1988**, *65*, 2664.